Wide-angle Polarization-independent Planar Magnetic Metamaterials Based on Dielectric Resonators

Jiafu Wang[1], **Shaobo Qu**[1,2], **Zhuo Xu**[2], **Hua Ma**[1], **Hongliang Du**[1], **Jun Wang**[1], **and Hongya Chen**[1]

[1]College of Science, Air Force Engineering University, Xi'an, Shaanxi 710051, China
[2]Electronic Materials Research Laboratory, Key Laboratory of the Ministry of Education
Xi'an Jiaotong University, Xi'an, Shaanxi 710049, China

Abstract— Based on dielectric resonators, the theory, design and implementation of planar magnetic metamaterials made of dielectric blocks were investigated. By etching simple metallic patterns on surface of the dielectric blocks, field distributions of the desired resonance modes can be enhanced while those of the undesired suppressed. In this way, the resonance frequency of the desired mode can be tuned down to lower frequency range. A wide-angle polarization-independent planar magnetic metamaterial based on short cylindrical dielectric resonators was proposed and analyzed. Due to its polarization-independence, wide incident angle, the magnetic metamaterial is ready to be used in various microwave components, such as antenna radomes, microwave filters and frequency selective surfaces.

1. INTRODUCTION

Metamaterials with negative permeability and/or negative permittivity have been attracting great attentions since the seminal work of Pendry and Smith [1, 2]. Due to unique electromagnetic properties, metamaterials have great potential application values in many fields. A great variety of metamaterials have been envisioned and fabricated. Similar to the working principle of SRR/Wire metamaterial, dielectric-metallic metamaterial unit cells, like S-shaped [3], Ω-shaped [4], coplanar magnetic/electric resonators [5], have been proposed. Nevertheless, there is an annoying problem for the above unit cells. Incident waves must be paralleled to the substrate plane, which make it quite troublesome to be fabricated and used. With an aim to overcome this problem, planar metamateirals, which allow the incident waves to be perpendicular to the substrate plane, were proposed and fabricated [6–11]. Typical planar metamaterials are the fishnet structures proposed by Soukoulis et al. [9].

Recently, many researchers are focusing on all-dielectric realization of metamaterials [12–18]. Many all-dielectric metamaterial unit cells, such as binary spherical [12], cubic [13] and disk-like unit cells [14], were proposed. These unit cells are based on different resonance modes in the unit cells which behave like dielectric resonators. Under a certain resonance mode, the effective permeability or/and permittivity are negative. The key to realizing all-dielectric metamaterials is to get the proper resonance modes. High-dielectric ceramics with good temperature stability and low dielectric loss are required to guarantee the long-wavelength condition. However, to date, dielectric constants of microwave ceramic materials, such as $Ba_2Ti_9O_{20}$, $BaTi_4O_9$, BaO-PbO-Nd_2O_3-TiO_2, are mostly between $30 \sim 100$, much less than some all-dielectric unit cells require [16, 17]. For many all-dielectric unit cells, their first resonance frequencies are so high that the long-wavelength condition cannot be met, so effective medium theory cannot be used to characterize them. As a result, it is desirable to design unit cells whose resonance modes can be tuned to lower frequencies.

In this paper, planar magnetic metamaterials based on practically-used dielectric resonators were proposed. As a typical example, magnetic metamaterials based on short cylindrical dielectric resonators were investigated. By etching a circular metallic ring on each end face of the dielectric resonator, the first resonance can be tuned significantly to lower frequency range so as to meet the long-wavelength condition. Thus, the magnetic metamaterial can be described by effective medium theory. Since the cross section of the dielectric resonator as well as the metallic ring are all circular, the magnetic metamaterial is independent of the polarization of incident waves. Under a wide incident angle range, the magnetic response keeps almost the same. Practical implementation of the proposed magnetic metamaterials was given. The proposed planar magnetic metamaterials owe its advantages to wide-angle incidence and polarization independence.

2. THEORY AND DESIGN

Only recently, materials having a dielectric constant between 30 and 100 with good temperature stability and low dielectric losses have become available. This greatly facilitate the design of practical all-dielectric metamaterials, but the dielectric constant of commercially available ceramic materials are still not so high as that required in some unit cells [16, 17]. This leads to a comparatively high resonance frequency. Thus, long-wavelength condition can not be satisfied and the corresponding metamaterials cannot be characterized by the effective medium theory. As a result, it is necessary to tune the desired resonance mode down to lower frequency ranges. All-dielectric metamaterials are always made of high-dielectric ceramic materials, no matter what shapes of the unit cells. A high-dielectric block can be regarded as a dielectric resonator, so we can design and tune the all-dielectric metamaterials by the same methods used in designing dielectric resonators.

For an isolated short cylindrical dielectric resonator shown in Fig. 1(a), the resonance mode with the lowest resonance frequency is the $TE_{0l\delta}$ mode. According to the electric and magnetic field distribution shown in Figs. 1(b) and (c), the resonators behaves like a magnetic dipole in $TE_{0l\delta}$ mode. Since the electric and magnetic dipole moments can be envisioned as the alphabet for making metamaterials [14], the resonator is expected to be a magnetic metamaterial in the $TE_{0l\delta}$ mode. Although the geometrical form of a dielectric resonator is extremely simple, an exact solution of the Maxwell equations is considerably more difficult than for hollow metal cavities. For this reason, the exact resonant frequency of a certain resonant mode, such as $TE_{0l\delta}$ mode, can only be computed by rather complicated numerical procedures. For an approximate estimation of the resonant frequency of the isolated dielectric resonator, the following simple formula [19] can be used

$$f_{\mathrm{GHz}} = \frac{34}{r_{\mathrm{mm}}\sqrt{\varepsilon_r}}\left(\frac{r}{h} + 3.45\right) \tag{1}$$

The radius of the resonator is denoted by r and its height by h. The lengths are expressed in millimeters, and the frequency in gigahertz. The relative dielectric constant of the material is ε_r. The above formula is accurate to about 2% in the range

$$0.5 < r/h < 2 \quad \text{and} \quad 30 < \varepsilon_r < 50 \tag{2}$$

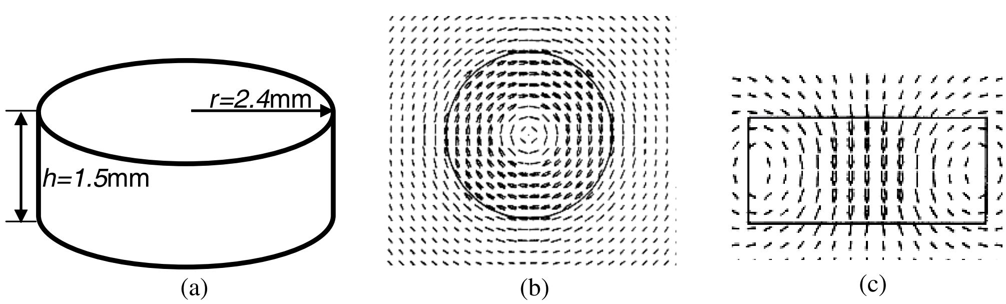

(a) (b) (c)

Figure 1: (a) An isolated short cylindrical dielectric resonator and (b) its electric field distribution in equatorial plane, (c) magnetic field distribution in meridian plane for $TE_{0l\delta}$ mode.

The dielectric resonator we consider in this paper as an example is made of $BaTi_4O_9$ whose dielectric constant $\varepsilon_r = 39.2$, loss angle tangent $\tan\delta = 0.0001$ and temperature coefficient $T_f = +4\,\mathrm{ppm}/^\circ\mathrm{C}$. The radius and height of the resonator are $r = 2.4\,\mathrm{mm}$ and $h = 1.5\,\mathrm{mm}$, respectively. By using (1) to estimate the first resonance frequency, we obtain

$$f_{\mathrm{GHz}} = \frac{34}{1.5 \times \sqrt{39.2}}\left(\frac{2.4}{1.5} + 3.45\right) \approx 18.3\,\mathrm{GHz}$$

At 18.3 GHz, the wave-length in free space is about 16.4 mm, less than four times the diameter of the resonator, so the unit cell cannot be described by effective medium theory. The resonance frequency of the $TE_{0l\delta}$ mode has to be tuned down.

Figure 2 shows the unit cell of the magnetic metamaterial. The unit cell is put into a $5\,\mathrm{mm} \times 5\,\mathrm{mm} \times 3\,\mathrm{mm}$ lattice. Compared with the dielectric resonator shown in Fig. 1(a), there are two thin circular copper rings on each end face of the dielectric resonator. The outer radius of the copper ring, the width and thickness of the copper strip are: $r_0 = 2.2\,\text{mm}$, $w = 0.2\,\text{mm}$, $t = 0.050\,\text{mm}$, respectively. From the electric and magnetic field distributions shown in Figs. 1(b) and (c), we can find that the electric field is stronger on the outer part of the end faces while the magnetic field is strongest in the center part around the axis. The copper ring is such that it is polarized along the electric field lines while perpendicular to the magnetic field lines. Thus, electric field on the end face and magnetic field pass through the copper ring all contribute to the enhancement of the magnetic resonance, so the copper ring can excite the $\text{TE}_{0l\delta}$ mode selectively. In contrast to the fact that the orientation of copper ring is along the direction of the electric field of $\text{TE}_{01\delta}$ mode, it is completely different from that of other higher order modes. As a result, the resonant frequency of $\text{TE}_{01\delta}$ mode will decrease significantly, whereas those of other modes will keep high.

3. SIMULATION RESULTS AND ANALYSIS

Numerical simulations were carried out using the commercial FDTD solver CST Microwave Studio. As shown in Fig. 2, the four lateral boundaries along x and y axes are Periodic Boundaries while the two boundaries along z axis are Open Boundaries. Plane waves are incident onto the unit cell with an incident angle θ with respect to the $-z$ direction.

Consider a normally incident plane wave onto the unit cell. Since the lateral boundaries are Periodic Boundaries, the structure is actually one layer of infinite magnetic metamaterial slab made of the unit cell shown in Fig. 2. Because the cross section of the dielectric resonator and the copper ring are all circular, the polarization of the incident plane wave has no influence on its magnetic response. Fig. 3 shows the simulated transmission spectra of one layer of the proposed magnetic metamaterial. As shown in Fig. 3, there is a transmission dip around 5 GHz. At 5 GHz, the wavelength in free space is about 60 mm, more than ten times larger the size of the unit cell, so effective medium theory can be employed. This means that we can use effective permeability and permittivity to describe the electromagnetic properties of the infinite magnetic metamaterial slab.

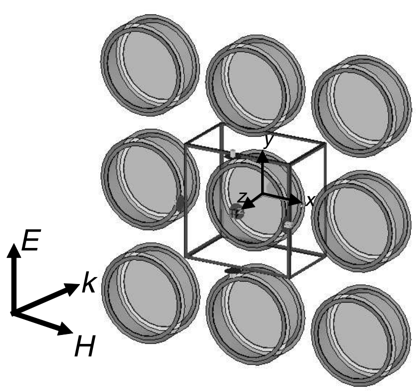

Figure 2: Unit cell of the planar magnetic metamaterial.

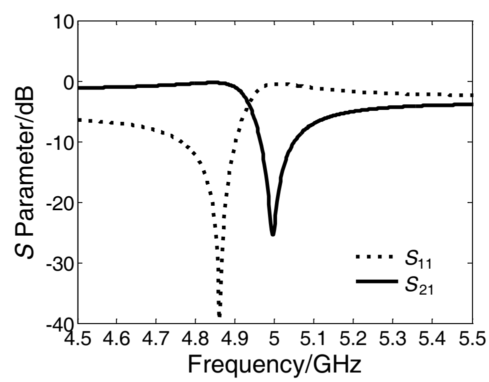

Figure 3: Transmission spectra under normal incidence.

The effective permeability and permittivity can be retrieved from S parameters obtained by simulations or experiments [20, 21]. Figs. 4(a) and (b) give the retrieved permeability and permittivity, respectively. Fig. 4(a) shows that the real part of effective permeability is negative from 4.95 GHz to 5.25 GHz. At the resonance frequency 4.95 GHz, there is a peak for the imaginary part of the effective permeability. In $4.95 \sim 5.05$ GHz, the imaginary part is negative while in $5.03 \sim 5.25$ GHz, the imaginary part is nearly zero. Since magnitude of the imaginary part is related to the magnetic loss, the magnetic loss is nearly zero in $5.05 \sim 5.25$ GHz. As to the effective permittivity, there is a corresponding anti-resonance [22] in $4.95 \sim 5.25$ GHz, as shown in Fig. 4(b).

For oblique incidences, we must consider two cases: incident TE plane waves and incident TM plane waves. In order to investigate the influence of the incidence angle, we can compare the transmission spectra under oblique incidences with that under normal incidence shown in Fig. 3. Since the transmission dip indicates a magnetic resonance, what we need to do is to see whether the dip varies greatly under different incidence angles. Figs. 5(a) and (b) show the transmission spectra under incident TE plane waves and incident TM plane waves, respectively. The incidence

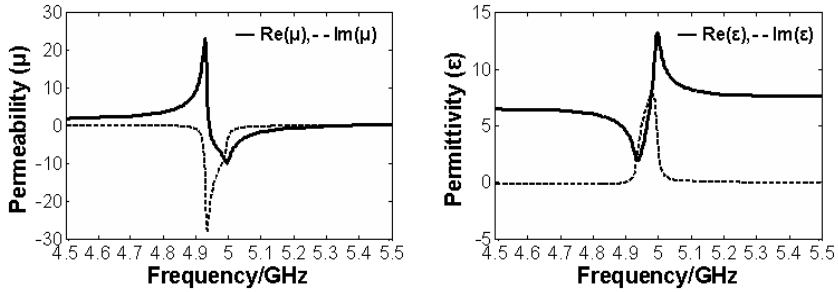

(a) (b)

Figure 4: Retrieved constitutive parameters: (a) effective permeability and (b) effective permittivity for one layer of the proposed magnetic metamaterial.

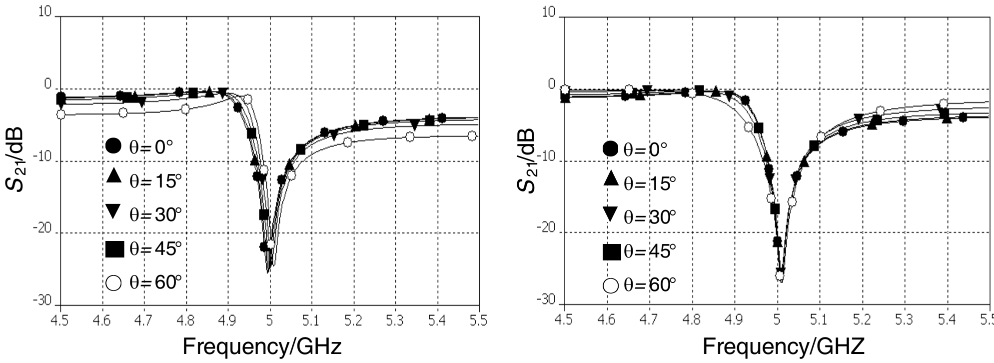

(a) (b)

Figure 5: Transmission spectra for (a) TE waves and (b) TM waves with incident angles between $0 \sim 60°$.

angles for the two cases vary from 0 to 60°. It is shown in Figs. 5(a) and (b) that the influence of incidence angles for both the TE and TM cases with incidence angles varying from 0 to 60° is so minor that the transmission dip almost keeps the same as that in normal incidence case. Thus, the magnetic resonance frequency keeps the same for varying incidence angles. Because negative effective permeability arises from the magnetic resonance, the frequency at which negative effective permeability starts is thus unchanged. Moreover, as the incidence angle increases, for the TE case, the upper part of the S_{21} curves bend lower than in the normal incidence case while for the TM case, the upper part of the S_{21} curves stand higher than in the normal incidence case. Since lower magnitude of S_{21} means lower transmission and thus wider bandwidth of negative permeability, as the incidence angle increases, the bandwidth of negative permeability in the TE cases becomes a bit wider than in the normal incidence case while in the TM case it becomes a bit narrower. However, the change of bandwidth with incidence angle is quite minor that we can approximately think that the bandwidth is the same as in the normal incidence case. From the above analysis, it can be concluded that the magnetic response of the proposed magnetic metamaterial keeps the same under a wide range of incidence angles.

3.1. Influences of Geometrical Parameters

For the proposed unit cell shown in Fig. 2, we use the copper ring to tune down the resonance frequency of $TE_{0l\delta}$ mode to realize negative permeability at much lower frequency range. Since the field intensity is different on different part of the dielectric resonator, the influence of copper ring is different when its geometrical parameters are changed. Thus, it is necessary to investigate the influence of its geometrical parameters. There are two main geometrical parameters for the copper ring: the outer radius and the strip width, so the influences of the two geometrical parameters were investigated.

Figures 6(a) and (b) show the transmission spectra under different outer radii and strip widths, respectively. As shown in Fig. 6(a), as the outer radius decreases, the transmission dip shifts to higher frequencies. This means that the resonance frequency of $TE_{0l\delta}$ mode increases as the outer radius decreases. This can be explained by the electric field distribution shown in Fig. 1(b). The electric field intensity is stronger on the outer part of the end face while weaker on the inner part.

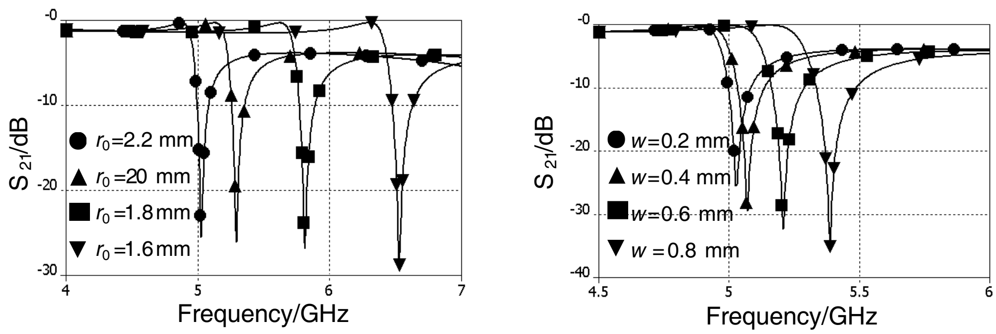

(a) (b)

Figure 6: Influences of (a) the outer radius of copper ring and (b) the width of copper strip.

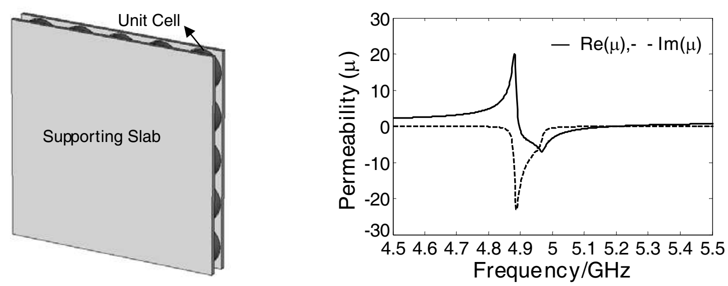

(a) (b)

Figure 7: Practical implementation of the proposed magnetic metamaterials: (a) fixing the unit cells by two supporting slab; (b) retrieved effective permeability of the structure.

When the outer radius of the copper ring reduces, the electric field coupling to the copper ring becomes weaker. Thus, higher frequency is needed to excite the $TE_{0l\delta}$ mode resonance. Fig. 6(b) shows that as the strip-width increases, the transmission dip blue-shifts, which means that the magnetic resonance frequency increases with the strip-width. As the strip-width increases, the coupling between the copper ring and the electric field of the dielectric resonator increases, which increases the electric energy while reduces the magnetic energy. Thus, the magnetic field is reduced as the strip-width increases. Again, higher frequency is needed to excite the $TE_{0l\delta}$ mode resonance.

4. PRACTICAL IMPLEMENTATION OF THE MAGNETIC METAMATERIAL

In practice, the unit cells have to be fixed. Some authors chose the method of embedding the high-dielectric blocks into low-dielectric matrix [12–14]. This method is demanding for the fabrication techniques and thus is difficult to use. To avoid such a difficulty, the planar magnetic metamaterial can be realized in practice by two supporting slabs, as shown in Fig. 7(a). In order to reduce the influence of the two supporting slabs, materials of supporting slabs must be with low dielectric loss and low dielectric constant. Teflon (PTFE) with a dielectric constant 2.08 and loss angle tangent 0.0004 is chosen to be the material of supporting slabs. Besides its low dielectric loss and low dielectric constant, the flexibility of Teflon is quite good, so the planar magnetic metamaterial can be bent freely, which makes it convenient to apply the planar magnetic metamaterial.

The influence of the two Teflon supporting slabs on the negative permeability was also investigated. For one layer of magnetic metamaterial shown in Fig. 7(a), the effective permeability is shown in Fig. 7(b). Compared with the effective permeability without supporting slabs shown in Fig. 4(a), the frequency range of negative real part of effective permeability, which has a red-shift, is now $4.9 \sim 5.2$ GHz. In $4.9 \sim 5.0$ GHz, the imaginary part is negative while in $5.0 \sim 5.2$ GHz it is zero. The bandwidth without magnetic loss is 0.2 GHz, the same as the case without supporting slabs.

5. CONCLUSIONS

According to the field distributions of different resonance modes of the dielectric resonator, metallic patterns can be etched on some special positions on the surface dielectric resonators to adjust the field distributions. Thus, the desired resonance mode can be enhanced while the undesired suppressed. As a result, resonance frequency of the desired modes will be reduced so as to meet the long wave-length condition. Metamaterials with negative permeability and/or negative permittivity can be realized by the desired resonance modes. Since there is a great many resonance modes for a given dielectric resonator, a great diversity of metamaterial can be designed based on different resonance modes. As a good example, a planar magnetic metamaterial based on short cylindrical dielectric resonators was designed and analyzed. The proposed planar magnetic metamaterial meets strictly the long wave-length condition and has almost the same electromagnetic response under a wide range of incidence angles. Because of its high flexibility, wide incidence angle range and polarization independence, the magnetic metamaterial is ready to be used in various microwave components, such as antenna radomes, microwave filters and frequency selective surfaces.

ACKNOWLEDGMENT

The authors are grateful to the supports from the National Natural Science Foundation of China under Grants Nos. 61331005, 11204378, 11274389, 11304393, 61302023, the National Science Foundation for Post-doctoral Scientists of China under Grant Nos. 2013M532131, 2013M532221, the Natural Science Foundation of Shaanxi Province under Grant Nos. 2011JQ8031, 2013JM6005, and the Aviation Science Foundation of China under Grant Nos. 20132796018 and 20123196015.

REFERENCES

1. Pendry, J. B., A. J. Holden, D. J. Robbins, and W. J. Stewart, *IEEE Trans. Microwave Theory Tech.*, Vol. 47, 2075, 1999.
2. Smith, D. R., W. J. Padilla, D. C. Vier, S. C. Nemat-Nasser, and S. Schultz, *Phys. Rev. Lett.*, Vol. 84, 4184, 2000.
3. Chen, H. S., L. X. Ran, J. T. Huangfu, X. M. Zhang, K. S. Chen, T. M. Grzegorczyk, and J. A. Kong, *Phys. Rev. E*, Vol. 70, 057605, 2004.
4. Ran, L., J. Huangfu, H. Chen, Y. Li, X. Zhang, K. Chen, and J. A. Kong, *Phys. Rev. B*, Vol. 70, 073102, 2004.
5. Wang, J. F., S. B. Qu, Z. Xu, J. Q. Zhang, Y. M. Yang, H. Ma, and C. Gu, *Photon. Nanostruct.: Fundam. Appl.*, Vol. 6, 183, 2008.
6. Zhou, J. F., L. Zhang, G. Tuttle, T. Koschny, and C. M. Soukoulis, *Phys. Rev. B*, Vol. 73, 041101, 2006.
7. Zhou, J. F., E. N. Economon, T. Koschny, and C. M. Soukoulis, *Opt. Lett.*, Vol. 31, 3620, 2006.
8. Alici, K. B. and E. Ozbay, *Photonics Nanostruct.: Fundam. Appl.*, Vol. 6, 102, 2008.
9. Kafesaki, M., I. Tsiapa, N. Katsarakis, T. Koschny, C. M. Soukoulis, and E. N. Economou, *Phys. Rev. B*, Vol. 75, 235114, 2007.
10. Guven, K., A. O. Cakmak, M. D. Caliskan, T. F. Gundogdu, M. Kafesaki, C. M. Soukoulis, and E. Ozbay, *J. Opt. A: Pure Appl. Opt.*, Vol. 9, 361, 2007.
11. Zhou, J. F., T. Koschny, L. Zhang, G. Tuttle, and C. M. Soukoulis, *Appl. Phys. Lett.*, Vol. 88, 221103, 2006.
12. Holloway, C. L., E. F. Kuester, J. Baker-Jarvis, and P. Kabos, *IEEE Trans. Antennas Propgat.*, Vol. 51, 2596, 2003.
13. Kim, J. and A. Gopinath, *Phys. Rev. B*, Vol. 76, 115126, 2007.
14. Ahmadi, A. and H. Mosallaei, *Phys. Rev. B*, Vol. 77, 045104, 2008.
15. Popa, B.-I. and S. A. Cummer, *Phys. Rev. Lett.*, Vol. 100, 207401, 2008.
16. Peng, L., L. X. Ran, H. S. Chen, H. F. Zhang, J. A. Kong, and T. M. Grzegorczyk, *Phys. Rev. Lett.*, Vol. 98, 157403, 2007.
17. Lepetit, T. and E. Akmansoy, *Microwave Opt. Tech. Lett.*, Vol. 50, 909, 2008.
18. Jylhä, L., I. Kolmakov, S. Maslovski, and S. Tretyakova, *J. Appl. Phys.*, Vol. 99, 043102, 2006.
19. Kajfez, D. and P. Guillon, 2nd Edition, Noble Publishing Corporation, Georgia, 1998.
20. Chen, X. D., T. M. Grzegorczyk, B.-I. Wu, J. Pacheco, Jr., and J. A. Kong, *Phys. Rev. E*, Vol. 70, 016608, 2004.
21. Smith, D. R., D. C. Vier, T. Koschny, and C. M. Soukoulis, *Phys. Rev. E*, Vol. 71, 036617, 2005.
22. Koschny, T., P. Markos, D. R. Smith, and C. M. Soukoulis, *Phys. Rev. E*, Vol. 68, 065602(R), 2003.